International Journal of Chemical, Materials and Biomolecular Sciences
ISSN: 2415-6620
Vol:14, No:11, 2020

Micromechanics of Stress Transfer across the Interface Fiber-Matrix Bonding

Fatiha Teklal, Bachir Kacimi, Arezki Djebbar

***Abstract*—**The study and application of composite materials are a truly interdisciplinary endeavor that has been enriched by contributions from chemistry, physics, materials science, mechanics and manufacturing engineering. The understanding of the interface (or interphase) in composites is the central point of this interdisciplinary effort. From the early development of composite materials of various nature, the optimization of the interface has been of major importance. Even more important, the ideas linking the properties of composites to the interface structure are still emerging. In our study, we need a direct characterization of the interface; the micromechanical tests we are addressing seem to meet this objective and we chose to use two complementary tests simultaneously. The microindentation test that can be applied to real composites and the drop test, preferred to the pull-out because of the theoretical possibility of studying systems with high adhesion (which is a priori the case with our systems). These two tests are complementary because of the principle of the model specimen used for both the first "compression indentation" and the second whose fiber is subjected to tensile stress called the drop test. Comparing the results obtained by the two methods can therefore be rewarding.

***Keywords*—**Interface, micromechanics, pull-out, composite, fiber, matrix.

I. Introduction

THE physicochemical aspect of composite interfaces is a difficult subject and our understanding of this feature is still far from complete. They are the theory of bonding at the fiber-matrix interface and the analytical techniques to characterize the interface. The nature or origin of the bonding between the fiber and matrix is discussed in terms of the theories of adhesion with associated mechanisms of bonding. The notion of interface or interphase remains relatively vague, as the interfacial zone does not exist in itself but is created during the implementation of the composite. Therefore, it appears very difficult to assign mechanical properties to it. One of the most important phenomena in FRCs is the stress transfer between the fiber and the matrix across the interphase/interface. When composites are subjected to various loading conditions, the efficiency of load transfer across the interface plays an important role in overall performance of the composites [1], [2]. However, these zones (interface/interphase) play a leading role, as shown by [3] and [4], since the interface and/or interphase ensure the transmission of the forces between the relatively soft matrix and the stiffer reinforcement. Consequently, the contribution of the reinforcement on the mechanical properties of the composite is directly related to the quality of the interfacial zone [5]. Kim et al. [6], [7] showed that a thorough understanding of the interfacial zone is considered as one of the criteria for composite design.

To develop tractable models, many researchers have modeled the interphase region as a homogeneous material [8]-[12]. However, a few studies considered the inhomogeneous nature of interphase adopting a stair-case variation of material properties across the thickness of the interphase layer [13], [14]. Alternatively, a few investigators proposed an effective interphase model (EIM) and uniform replacement model (URM) to replace the fiber and the surrounding interphase by an effective homogeneous fiber in order to convert a three-phase composite into a two-phase composite [15]. For mathematical convenience and to better describe the variation of properties within the interphase region, several researchers treated the interphase as an inhomogeneous material by smoothly varying the material properties as a function of radius. Usually in such models, the material properties are graded by adopting an empirical law [16]-[21].

II. Principle and Interest of the Drop Test

The drop test is different from that of heaving the particular configuration of the samples: here, the fiber is embedded in a resin micro drop deposited on the monofilament before cooking. During the tensile test, it is maintained by using two plates (Fig. 1 (a)). The only limiting factor is the test, in the case of a thermosetting resin, the initial viscosity of the resin, if it is too high, prevents the deposition of small drops. Finally, the drop test allows, from the pull-out, achieving relatively fast for a large number of samples (the implementation of these do not require specific mounting) [22]. Fig. 1 (b) shows the curves obtained from tensile testing of gout. As in pull-out, these curves to determine the strength of groundwood F_d. The whole problem is then to relate this experimental scale to a specific parameter of the interface [23]-[25].

A. Geometry of the Drop and Put into Equation

It appears that the actual geometry of the test can be modeled as shown in Fig. 1 (a), a cylinder of length L

Fatiha Teklal was with the Mechanics, Structures and Energetics Laboratory (L.M.S.E), University of Mouloud MAMMERI on Tizi Ouzou, BP 17 RP 15000, Tizi Ouzou, Algeria (corresponding author, phone: 213 663 255 507: e-mail: fatihagm07@yahoo.fr).

Bachir Kacimi is with the Mechanics, Structures and Energetics Laboratory (L.M.S.E), University of Mouloud MAMMERI on Tizi Ouzou, BP 17 RP 15000, Tizi Ouzou, Algeria (phone: 213 771 771 122; e-mail: kacimiummto@yahoo.fr).

Arezki Djebbar is with the Mechanics, Structures and Energetics Laboratory (L.M.S.E), University of Mouloud MAMMERI on Tizi Ouzou, BP 17 RP 15000, Tizi Ouzou, Algeria (phone: 213 555 274 501; e-mail: ar.djebbar@yahoo.fr).

represents Gout, or L is the length of entrenchment, but the length of the drop. Index, "m", "f", refers to the matrix and the fiber, τ means the shear stress at the interface that is to say ρ = r. We put in elastic, linear, with axial symmetry (no twist). We assume that the axial stresses in the matrix σ_m, and in the fiber σ_f, radial effects are negligible. These effects include swelling of the matrix and fiber contraction due to the effects of Poisson's ratio.

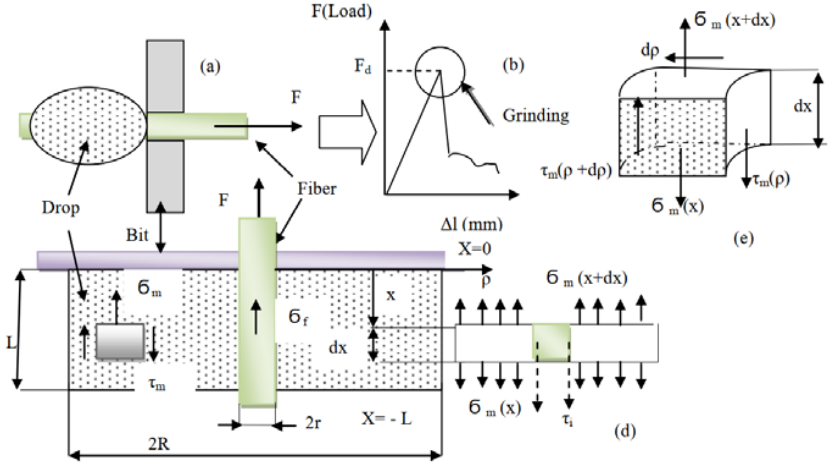

Fig. 1 Model of the drop/Fiber (a); load- displacement curve (b); balance of forces on a section (c), (d) and (e)

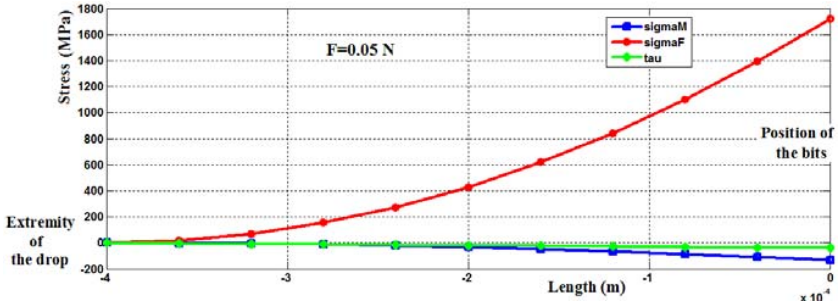

Fig. 2 Evolution constraints [$\sigma_f, |\sigma_m|, |\tau_i|$] based on the embedded length for an applied force of 0.05 N (drop test, epoxy/glass)

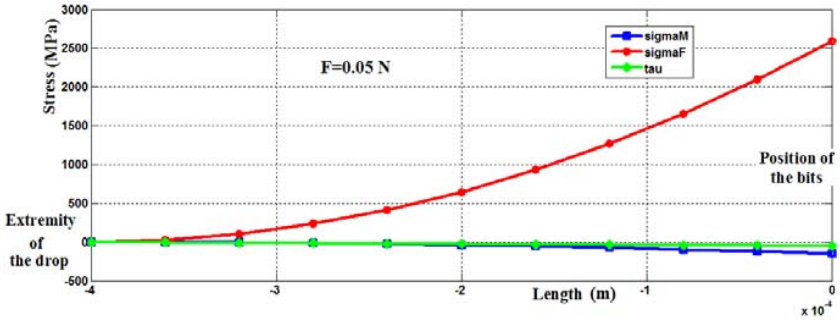

Fig. 3 Evolution constraints [$\sigma_f, |\sigma_m|, |\tau_i|$] based on the embedded length for an applied force of 0.05 N (drop test, couples epoxy/carbon)

B. Setting Equation

Let us now apply the balance of forces on various parts of the system, Fiber + drop (Fig. 1 (a)). Writing the balance of a fiber section leads to (1):

$$F = \int_{x=-L}^{x=0} (2\pi r)\tau_i(x)dx \tag{1}$$

$$\frac{d\sigma_f}{dx} = \frac{2\tau_i(x)}{r} \tag{2}$$

$$\tau_i'' - \alpha^2 \tau_i = 0 \tag{3}$$

The resolution of (3) gives the evolution of shear stresses at the fiber/matrix interface τ_i (x), the normal stress at the fiber

level σ_f and at the matrix level σ_m are given by (4)-(6) respectively:

$$\tau_i(x) = \frac{-\alpha F}{2\pi r\left(ch(\alpha L)-1\right)} sh\left[\alpha\left(x+L\right)\right] \quad (4)$$

$$\sigma_f = \frac{F\left[ch\left(\alpha\left(x+L\right)\right)-1\right]}{\pi r^2\left[ch(\alpha L)-1\right]} \quad (5)$$

$$\sigma_m = \frac{-F\left[ch\left(\alpha\left(x+L\right)\right)-1\right]}{\pi\left(R^2-r^2\right)\left[ch(\alpha L)-1\right]} \quad (6)$$

For our simulation we used a calculation software MATLAB. The evolution of the stress profile $[\sigma_f, |\sigma_m|, |\tau_i|]$ as a function of the embedded length for the different values of the applied load is shown in Figs. 2 and 3. We chose for our simulation; thermosetting epoxy matrix (drop) in diameter, 2R = 30 µm with mechanical properties E_m = 4.5 GPa, G_m = 1.6 GPa and two types of E-glass filament (r = 4 µm, E_f = 73 GPa) and carbon-HT (r = 3.5 µm, E_f = 230 GPa).

The evolution of profile of the stresses $[\sigma_f, |\sigma_m|, |\tau_i|]$ according to the length enchased for the various values of the load applied are represented by Figs. 2 and 3. From the plotted curves we find that evolutionary constraints $[\sigma_f, |\sigma_m|, |\tau_i|]$ are the same for both types of fiber (carbon, glass). The value of the stress σ_m of the matrix and shearing of the interface τ_i varies in a decreasing way with the length of the enshrining until they become null; same for the longitudinal stress fiber σf which decreases with the length embedded. Through the results obtained for the test of drop, we could highlight:

The high values of τ_i obtained for the various couples (carbon/epoxy, glass/epoxy) are not due to a bad evaluation of τ_i nor even to a numerical overvaluation of the force applied. It is for this reason that the rupture occurs at the interface rather than in the matrix (for lengths of 45 µm to 125 µm entrenchment). Several explanations can be raised: It appears that the shear stress decreases rapidly away from that of the fiber; this then means that only the interfacial zone is subject to strong constraints, and this could pose a greater resistance than the matrix. According to the results we see three cases:

- For the first case when $\tau_i > \sigma_m$ two cases may appear, strong adhesion of the material tested, or due to modeling error. The characteristics of the interface are higher than those of the matrix and it is the properties thereof that limit the behavior of the composite. In this case we cannot characterize the interface and this case is not real.
- For the 2nd case $\tau_i \approx \sigma_m$ values of the embedding length range from 135 µm to 150 µm; the two curves show the stress at the interface and the normal stress at the matrix are close to the two lines of evolution and superimposed. In this case the interface behavior follows that of the matrix.
- For the 3rd case $\tau_i < \sigma_m$ lengths embedding 400 µm to 175 µm variants of σm values obtained for the matrix are larger than the interface; the characteristics of the interface are lower than those of the matrix and thus constitute the weak point at the origin of the rupture; this is the case we will consider in the tests because it represents the reality.

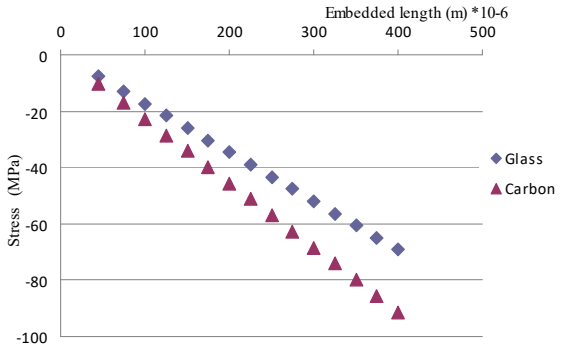

Fig. 4 Evolution of maximum interfacial stresses as a function of embedded length for a constant force F = 0.09 N for the drop test

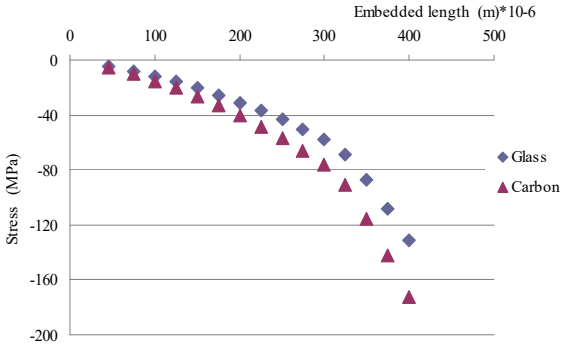

Fig. 5 Evolution of maximum interfacial shear stress as a function of embedded length

The maximum stresses at the interface for a constant force of 0.075 N and 0.09 N evolve linearly with the length embedded, such as the shear stress $\tau_{i,max}$ is high for carbon/ epoxy (Figs. 4 and 5). The stresses operate in the same way for the two couples, and the maximum stress is more important for carbon/epoxy (Fig. 5). These values are indeed greater than the shear strength of epoxy τ = 80 MPa; if they represented really interfacial resistance, an interfacial failure could occur, matrix having sold well before. However, we can wonder whether the value of τ, determined by a macroscopic mechanical test on pure resin, really corresponds to resistance to local intrinsic rupture of material. In a massive test-tube, the final rupture generally intervenes by the propagation of a fissure started on a defect, however, in the vicinity of this defect, leading to the rupture of material is much higher than the measured nominal stress. The apparent discrepancy between our estimate of the interfacial strength and matrix strength is probably less important than it seems.

III. Principle and Interest of Indentation Test

The micro-indentation test allows a measure of the force of cohesion in situ real composite (mainly one-way). This method currently has a process of taking action and fully automated data acquisition [26]. It requires the polishing of samples of composites having fibers perpendicular to the surface, and consists of driving, using an indenter on the end of a fiber to fiber debonding of the sheath matrix, to access a feature of the fiber/matrix interface. The final docking of the indenter in the surrounding matrix constitutes a criterion for stopping the test [25], [27].

The stress measurement of decohesion σ_d then makes it possible to deduce interfacial resistance to the shearing τ_i which is a rather complex function of σ_d, elastic characteristics G_m of the matrix and E_f of fiber, diameter d of fiber and distance interfibres T_m (Figs. 6, 7) [23].

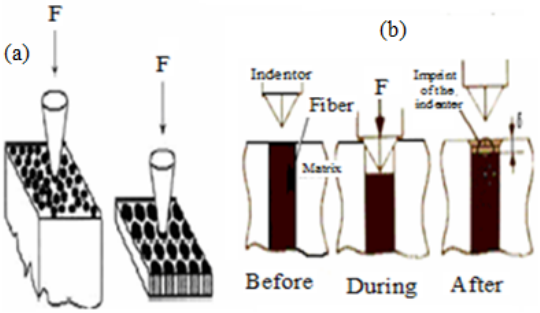

Fig. 6 (a) test of Indentation, (b) Schematic of the indentation test according to [28]

A. Analytical Modeling

In this model, we have developed an analytical approach that is simpler to implement than in the numerical method and that allows a more direct interpretation of the physical phenomena that are supposed to take place during the tests [28]. The model was based on [29], which already took into account the effect of inter-fiber distance in the composite specimen. The Piggott model has been modified by introducing loading conditions and boundary conditions representative of the test conditions. We have considered a perfect hexagonal arrangement of fibers and introduced the notion of equivalent radius, R_{eq}, to reduce the initial geometry to an equivalent value (Fig. 8) (the introduced geometry is an axisymmetric model formed of concentric cylinders).

The equivalent radius is defined by: $\pi R_{eq}^{\ 2} - \pi r^2 = A$

where r is the fiber radius and A is the matrix area contained in the circle of radius R.

It is assumed that the longitudinal displacement is zero at the "equivalent" fiber/matrix interface (at a distance Req) since tests showed that the bordering fibers did not move and that the interfaces were not damaged. Using Piggott's approach, this leads to the differential equation (7):

$$\frac{d^2\sigma_f}{dx^2} = \frac{n^2}{r^2}\sigma_f \tag{7}$$

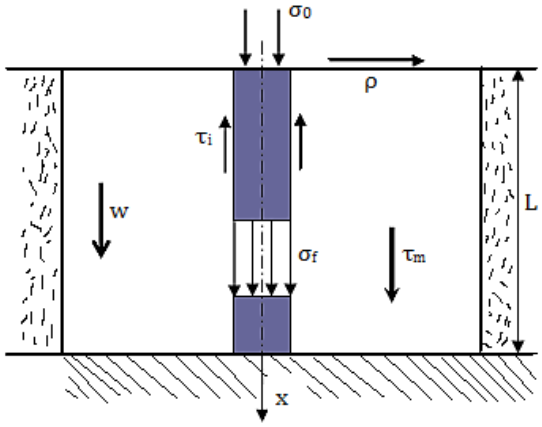

Fig. 8 Equivalent geometry (section)

where

$$n^2 = \frac{2G_m}{E_f Ln\left(\frac{R_{eq}}{r}\right)}$$

σ_f is the fiber longitudinal stress, E_f the fiber Young's modulus and G_m the matrix shear modulus. The solution is done from (8):

$$\sigma_f = Bsh(nx/r) + Dch(nx/r) \tag{8}$$

To write the boundary conditions, it is assumed first that σf is homogeneous on a section of fiber (even on the upper surface) and second that L >> R, where L is the thickness of the sample. We obtain at x=0, $\sigma_f = \sigma_0 = -F/\pi r^2$ and at x=L, $\sigma_f = 0$. Thus (9):

$$\sigma_f = -\sigma_0\left[ch\left(\frac{nx}{r}\right) - \coth\left(\frac{nL}{r}\right)sh\left(\frac{nx}{r}\right)\right] \tag{9}$$

If τ_i is the interfacial shear stress, then the equilibrium force on a fiber section leads to (10):

$$\tau_i = -\frac{r}{2}\frac{d\sigma}{dx} \tag{10}$$

This gives (11):

$$\tau_i = \frac{n\sigma_0}{2}\left[sh\left(\frac{nx}{r}\right) - \coth\left(\frac{nL}{r}\right)ch\left(\frac{nx}{r}\right)\right] \tag{11}$$

τ_i is maximum at x = 0 and $\tau_{i\max} = \frac{n\sigma_0}{2}\coth\left(\frac{nL}{r}\right)$ and as $L/r \to \infty : \tau_{i\max} = \frac{n\sigma_0}{2}$ (indeed, experimentally L = 1 cm and R

= 10 µm). Then, for F = F_d, $\tau_{i\max} = \tau_i$, where τ_i is the interfacial shear strength (12); thus:

$$\tau_i = \frac{F_d}{2\pi r^2}\sqrt{\frac{2G_m}{E_f Ln\left(\frac{R_{eq}}{r}\right)}} \quad (12)$$

B. Determination of R_{eq}

The real neighborhood of a fiber is different from the idealized case: the nearest fibers are positioned at various distances and generally, they do not have the same diameter. The tests performed induce only a partial debonding of each indented fiber; this means that the model presented above can be applied. The equivalent radius, R_{eq}, is then defined (13):

$$\frac{\theta R_{eq}^2}{2} = \frac{\theta r^2}{2} + A_m \text{ or by } \frac{\theta R_{eq}^2}{2} = \frac{\theta R^2}{2} - A_f \quad (13)$$

Am (resp. A_f) is the area of matrix (resp. of fiber) included in the sector of angle θ and radius R (Fig. 9). A_f is approximated by (14):

$$A_f = \frac{(\pi-\theta)c^2}{2} + cR\left(1-\cos\left(\frac{\theta}{2}\right)\right) \quad (14)$$

so:

$$R_{eq}^2 = R^2 + c^2 - \frac{2cR}{\theta}\left(1-\cos\left(\frac{\theta}{2}\right)\right)$$

where

$$\theta = 2Arc\sin\left(\frac{c}{R}\right) \quad (15)$$

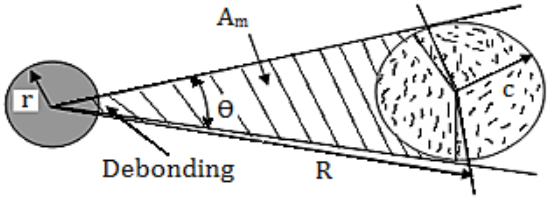

Fig. 9 Local determination of the equivalent radius

For our simulation we used a computation software MATLAB. The graphical representation of the stresses given by (9) and (11) are shown in Fig. 10. For our calculation we have chosen an epoxy thermohardening matrix, with mechanical properties E_m = 4.5 GPa, G_m = 1.6 GPa, and two types of glass E fiber (r = 4 µm, E_f = 73 GPa) and carbon HT (r = 3.5 m, E_f = 230 GPa). We varied the length of embedding tests of 45 µm to 400 µm, the loads applied maximum F_d of 0,05 N to 0,17 N and the radius equivalent to the radius of the fiber (Req/r) from 2,3 to 6,93.

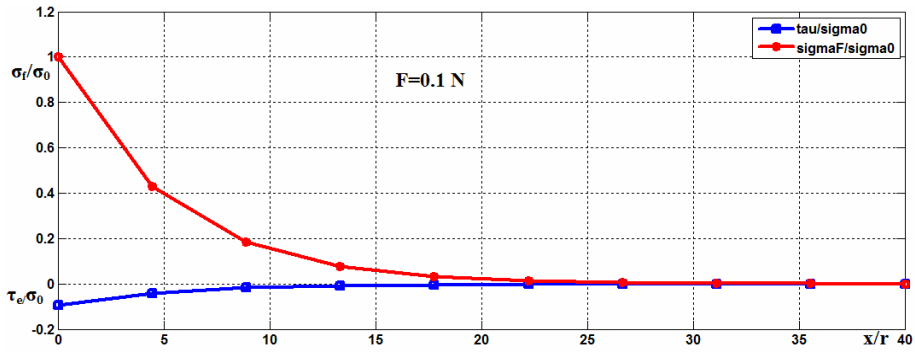

(a)

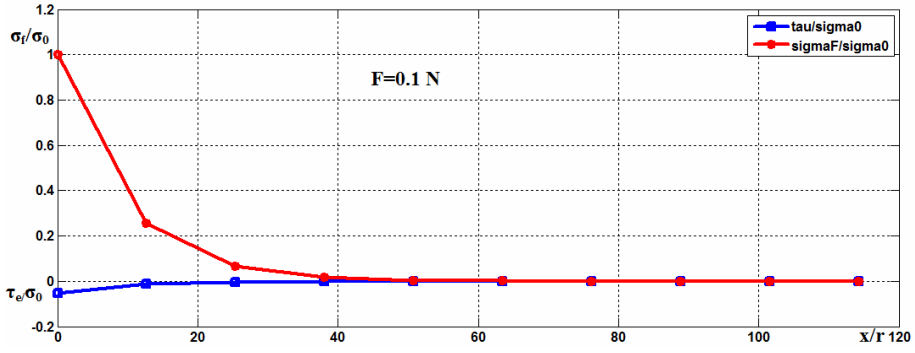

(b)

Fig. 10 Profile of the stresses in a test of indentation for fiber glass (a) and carbon (b) of Req/r = 2.3 and F = 0.1 N, L = 400 µm

From the plotted curves we see that the evolution of stress ratio and depending on the ratio x/r is the same for both types of fibers (carbon, glass). In the light of the results obtained for the test of indentation of the two material couples, we have to raise the following observations: The value of the ratio of shear stress at the interface/strain at the top of the fiber (τ_i/σ_0) varies in a manner with decreasing the ratio of embedded length/radius of the fiber (x/r) until they become null; same for the value of the ratio of the longitudinal stress of the fiber/ stress at the top of the fiber ($\sigma_f\ \sigma_0$) which decreases the ratio of embedded length/radius of the fiber (boundary conditions).

The simulated tests with variable load (F = 0,05N to 0,17N) highlighted the existence of a grinding force (F_d) strength below which no slippage of the fiber is possible. One can see results of test of microindentation simulated for the two couples of samples of composite (glass/epoxy, carbon/epoxy). This force of separation (F_d) is a parameter essential and present the force necessary to break the interfacial connection fiber/matrix; indeed, the fiber/matrix couples chosen in our study show strong interfacial adhesion. It is thus necessary to break this bond before inducing any interfacial slip.

From the plotted curves (Fig. 10) we note that the influence of interfiber distance is clear that, if the aforementioned decreases, the same fiber displacement results in a higher shear rate, therefore a higher interfacial shear stress, so debonding will be observed more easily than in the case of a strong matrix layer interfibre especially in the case of materials with glass fiber. We note that the values of the interfacial stresses obtained are higher for the couple glass/epoxy than for carbon/epoxy. The analytical modeling, which we developed, thus, is adapted perfectly to the characterization of the composites with carbon and glass fibers for the test of indentation.

IV. Conclusion

Micromechanical tests developed so far have kept a share of simplicity and specific characteristics; such as type of stress, the dimension and nature of specimens and the boundary conditions. These tests allow a qualitative study of the interface. Based on these tests, interface stands for values below the calculated interfacial resistance but the reality is that the interface will resist for values lower than the calculated interfacial resistance allow a qualitative study of the interface but reality shows that this interface is damaged at values much lower than these values, so other parameters can intervene in the case of finished products. In addition, it will optimize couples reinforcements/matrix and determine the effect of surface treatment of the reinforcement.

References

[1] Kim, J.K., Mai, Y.W., 1998. Engineered Interfaces in Fiber Reinforced Composites. Elsevier Science.
[2] Jiang Xiaoyu, KONG Xiangan, Micro-mechanical characteristics of fiber/matrix interface in composite materials, Composites Science and Technology 59(1999) 635-642.
[3] Drzal L. T. the Interphase in Epoxy Composites , Advances in Polymer Science, Editor: K. Dušek 1986; vol.75: pp 1-32.
[4] M.R. Piggott, The Effect of the Interface/interphase on Fiber Composite Properties, polymer Composites, October 1987, Volume 8, Issue 5, pages 291–297, (Version of Record online: 30 AUG 2004).
[5] J.K. Kim & Y.W. Mai, High Strength, High Fracture Toughness Fibre Composites with Interface Control A Review, Composites Science and Technology 1991; 41: 333-378.
[6] J. K. Kim, L. Zhou, Y.W. Mai / Stress transfer in the fiber fragmentation test- Part I An improved analysis based on a shear strength criterion/ Journal of Materials Science 1993; 28: 6233-6245.
[7] J. K. Kim, Y.W. Mai, Stress transfer in the fiber fragmentation test- Part II Multiple fiber composites, Journal of Materials Science 1995; 30: 3024-3032.
[8] Christensen, R., Lo, K., 1979. Solutions for effective shear properties in three phase sphere and cylinder models. J. Mech. Phys. Solids 27 (4), 315–330.
[9] Hashin, Z., 1990. Thermoelastic properties of fiber composites with imperfect interface. Mech. Mater. 8 (4), 333–348.
[10] Hayes, S., Lane, R., Jones, F., 2001. Fibre/matrix stress transfer through a discrete interphase. Part 1: single-fibre model composites. Compos.Part A Appl. Sci. Manuf. 32 (3), 379–389.
[11] Qiu, Y., Weng, G., 1991. Elastic moduli of thickly coated particle and fiber reinforced composites. J. Appl. Mech. 58 (2), 388–398.
[12] Rjafiallah, S., Guessasma, S., Bizot, H., 2010. Effect of surface etching on interphase and elastic properties of a biocomposite reinforced using glass–silica particles. Compos. Sci. Technol. 70 (8), 1272–1279.
[13] Jiang, Y., Guo, W., Yang, H., 2008. Numerical studies on the effective shear modulus of particle reinforced composites with an inhomogeneous inter-phase. Comput. Mater. Sci. 43 (4), 724–731.
[14] Wang, J., Crouch, S.L., Mogilevskaya, S.G., 2006. Numerical modeling of the elastic behavior of fiber-reinforced composites with inhomogeneous interphases. Compos. Sci. Technol. 66 (1), 1–18.
[15] Shen, L., Li, J., 2005. Homogenization of a fibre/sphere with an inhomogeneous interphase for the effective elastic moduli of composites. Proc. R. Soc. A Math. Phys. Eng. Sci. 461 (2057), 1475–1504.
[16] Jayaraman, K., Reifsnider, K.L., 1992. Residual stresses in a composite with continuously varying Young's modulus in the fiber/matrix interphase. J. Compos. Mater. 26 (6), 770–791.
[17] Jayaraman, K., Reifsnider, K.L., 1993. The interphase in unidirectional fiber-reinforced epoxies: effect on residual thermal stresses. Compos. Sci. Technol. 47 (2), 119–129.
[18] Huang, Y., Young, R.J., 1996. Interfacial micromechanics in thermoplastic and thermosetting matrix carbon fibre composites. Compos. Part A Appl. Sci. Manuf. 27 (10), 973–980.
[19] Kiritsi, C., Anifantis, N., 2001. Load carrying characteristics of short fiber composites containing a heterogeneous interphase region. Comput. Mater. Sci. 20 (1), 86–97.
[20] Shen, L., Li, J., 2003. Effective elastic moduli of composites reinforced by particle or fiber with an inhomogeneous interphase. Int. J. Solids Struct. 40 (6), 1393–1409.
[21] Romanowicz, M., 2010. Progressive failure analysis of unidirectional fiber-reinforced polymers with inhomogeneous interphase and randomly distributed fibers under transverse tensile loading. Compos. Part A Appl. Sci. Manuf. 41 (12), 1829–1838.
[22] P.S.Theocaris «The unfolding model for the representation of the mesophase layer in composites (Representation de la mésophase des composites par un modèle de transition) ». Journal of Applied Polymer Science, 30, p. 621-645, New York (1985).
[23] Allen Yu, Vijay Gupt «Measurement of in situ fiber/matrix interface strength in graphite/epoxy composites. University of California (1998).
[24] A. Kelly, W.R. Tyson « fiber strengthened materials, in high strength material». V.F, Zackay Ed, J. Wiley &Sons, London (1964).
[25] N. Chandra, H. Ghonem Interfacial mechanics of push-out tests: «theory and experiments». Composites part A: applied science and manufacturing (2001).
[26] Ibrahim Mohamed Haisam « Elaboration des matériaux composites modèles unifilamentaire à fibres longues et matrice silice sol-gel et caractérisation micromécaniques de l'interface». Thèse de doctorat, Ecole Doctorale Matériaux de Lyon (2006).
[27] Gutowski (W) Effet of fibre -matrix adhésion on mechanical properties of composites (effet de l'adhésion fibre-matrice sur les propriétés mécaniques des composites P505-520, composites interfaces (ICC-III), Elsevier science, Pub.CO, Inc, New York (1990).
[28] Béatrice Large –Toumi Etude du comportement en fatigue de composite carbone époxyde : rôle de l'interface Thèse de doctorat école centrale de LYON (1994).